Journal of Arrhythmia 33 (2017) 214–219

Contents lists available at ScienceDirect

Journal of Arrhythmia

journal homepage: www.elsevier.com/locate/joa

Original article

Influence of myopotential interference on the Wavelet discrimination algorithm in implantable cardioverter-defibrillator

Kazuya Mizukami, MD, PhD[a], Hisashi Yokoshiki, MD, PhD[b,*], Hirofumi Mitsuyama, MD, PhD[b], Masaya Watanabe, MD, PhD[b], Taro Tenma, MD[b], Rui Kamada, MD[b], Masayuki Takahashi, MD[b], Ryo Sasaki, CE[c], Motoki Maeno, CE[c], Hiroyuki Tsutsui, MD, PhD[b]

[a] Department of Cardiovascular Medicine, National Hospital Organization Hokkaido Medical Center, Yamanote 5-7-1-1, Nishi-ku, Sapporo 063-0005, Japan
[b] Department of Cardiovascular Medicine, Hokkaido University Graduate School of Medicine, Kita-15, Nishi-7, Kita-ku, Sapporo 060-8638, Japan
[c] Division of Medical Engineering Center, Hokkaido University Hospital, Japan

ARTICLE INFO

Article history:
Received 23 June 2016
Received in revised form
1 August 2016
Accepted 26 August 2016
Available online 1 October 2016

Keywords:
Implantable cardioverter-defibrillator
Tachycardia discrimination
Morphology
Myopotential interference
Wavelet

ABSTRACT

Background: Wavelet is a morphology-based algorithm for detecting ventricular tachycardia. The electrogram (EGM) source of the Wavelet algorithm is nominally programmed with the Can-RV coil configuration, which records a far-field ventricular potential. Therefore, it may be influenced by myopotential interference.
Methods: We performed a retrospective review of 40 outpatients who had an implantable cardioverter-defibrillator (ICD) with the Wavelet algorithm. The percent-match score of the Wavelet algorithm was measured during the isometric chest press by pressing the palms together. We classified patients with percent-match scores below 70% due to myopotential interference as positive morphology change, and those with 70% or more as negative morphology change. Stored episodes of tachycardia were evaluated during the follow-up.
Results: The number of patients in the positive morphology change group was 22 (55%). Amplitude of the Can-RV coil EGM was lower in the positive morphology change group compared to that in the negative group (3.9 ± 1.3 mV vs. 7.4 ± 1.6 mV, P=0.0015). The cut-off value of the Can-RV coil EGM was 5 mV (area under curve, 0.89). Inappropriate detections caused by myopotential interference occurred in two patients (5%) during a mean follow-up period of 49 months, and one of them received an inappropriate ICD shock. These patients had exhibited positive morphology change.
Conclusions: The Wavelet algorithm is influenced by myopotential interference when the Can-RV coil EGM is less than 5 mV.

1. Introduction

The implantable cardioverter-defibrillator (ICD) has become a standard therapy for the prevention of sudden cardiac death in patients with lethal ventricular arrhythmias [1,2]. It has been reported that ICD can also reduce the mortality in patients at risk of such arrhythmias [1–4]. Therefore, ICD implantation continues to be commonly performed.

Inappropriate ICD shocks, most frequently caused by supraventricular tachyarrhythmias [5,6], are not rare [5–8], despite effective device-related discrimination methods such as dual-chamber ICDs [9,10] and the stability/sudden-onset detection [11,12]. Since inappropriate shocks could result in poorer quality of life [13,14], proarrhythmia [15–17], and increased mortality, [5,7] improvements in tachyarrhythmia detection algorithms in ICD devices are required.

Wavelet™ (Medtronic Inc., MN, USA) is one of the morphology-based algorithms that prevent inappropriate ICD therapy due to supraventricular tachycardia (SVT) [18]. It was reported that the Wavelet algorithm effectively distinguishes SVT from ventricular tachycardia (VT) [18,19]. However, since Wavelet is a morphology-based algorithm, its accuracy of discrimination depends on the quality of electrogram (EGM).

The EGM source of the Wavelet algorithm is nominally programmed with the Can-RV coil configuration. It uses a far-field EGM, which is superior to near-field EGM in VT detection [20,21]. In addition, it was reported that the morphology of the Can-RV coil EGM was stable across different body positions, thereby maintaining the high percent-match score on the Wavelet algorithm [22–24]. On the other hand, the far-field EGM obtained by the

* Corresponding author. Fax: +81 11 706 7874.
E-mail address: yokoshh@med.hokudai.ac.jp (H. Yokoshiki).

http://dx.doi.org/10.1016/j.joa.2016.08.005
1880-4276/

Can-RV coil configuration may be influenced by myopotential interference.

The aim of this retrospective study was to evaluate the influence of myopotential interference on the Wavelet algorithm in patients with an ICD.

2. Materials and methods

2.1. Subjects

We performed a retrospective review of 43 consecutive outpatients who received an ICD with the Wavelet algorithm and visited Hokkaido University Hospital from April 2013 to August 2013. Three patients were excluded from analysis because of data insufficiency.

The baseline Can-RV coil EGM was obtained usually during sinus rhythm at rest and was stored as a template. The percent-match score on the Wavelet algorithm, which would represent the degree of morphologic similarity from the baseline EGMs, was measured during isometric chest press by pressing the palms together [25,26]. This maneuver was the most sensitive provocative test for myopotential interference in patients with a permanent unipolar pacemaker [25]. We classified patients with percent-match scores below 70% due to myopotential interference as positive morphology change, and those with 70% or more as negative morphology change. The cut-off value of 70% is the nominal value to discriminate VT from supraventricular tachyarrhythmias [18,22].

In most cases, the VF zone detected ventricular events faster than 185–200 beats/min, while the VT zone detected ventricular events faster than 150–170 beats/min. In cases of patients with documented slow VT, the detection zone lower than 150 beats/min was sometimes programmed [6].

The study was approved on September 20, 2012, by the Ethics Committee of Hokkaido University Hospital (approval number: 012-0156 and 016-0118).

2.2. Data acquisition

For each patient, baseline data at the time of ICD implantation were collected from medical records. These included demography, underlying heart diseases, heart failure status, comorbidities, and medications. Left ventricular ejection fraction was measured by echocardiogram. The ICD parameters were measured at each outpatient visit (every 3–4 month). The data regarding the amplitude of Can-RV coil EGM and the percent-match score on the Wavelet algorithm during the isometric chest press were collected during the outpatient visits from April 2013 to August 2013. Stored episodes of tachycardia were collected at the regular follow-up visits and each visit prompted by ICD therapy. Data from the day of ICD implantation to the end of March 2015 were collected.

2.3. Statistical analysis

Continuous variables were presented as mean ± SE (standard error) and categorical variables as number and percentage. Simple between-group analysis was conducted using Student's t-test, while categorical variables were compared using Fisher's exact test. To evaluate the predictors of positive morphology change during the isometric chest press, we used logistic regression analyses. For the model selection, we used stepwise logistic regression procedures (model entry $P < 0.05$ and removal $P > 0.1$). The sensitivity and specificity of amplitude of Can-RV coil EGM for its prediction were evaluated using the receiver operating characteristic (ROC) curve. Differences with $P < 0.05$ were considered significant. JMP® 10 (SAS Institute Inc., Cary, NC, USA) was used for all statistical analysis.

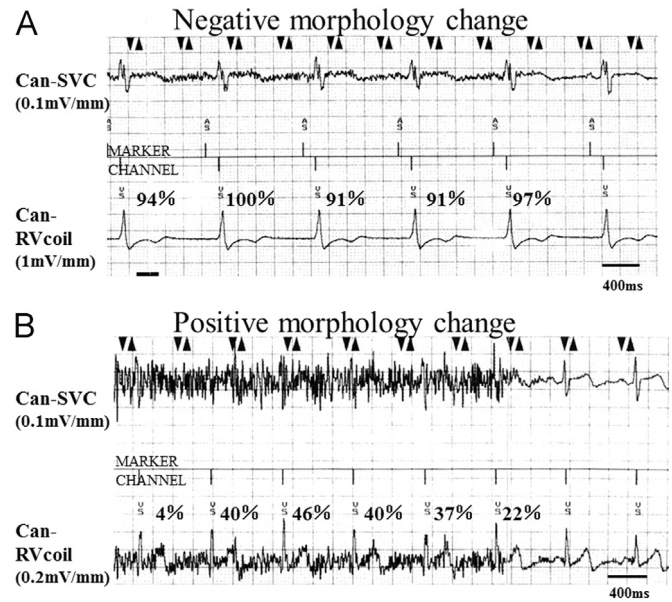

Fig. 1. Electrograms (EGMs) during the isometric chest press. Representative EGMs from negative morphology change (A) and positive morphology change (B) are shown. The isometric chest press was achieved by pressing the palms together. % is the percent-match score of the Can-RV coil EGM on the Wavelet algorithm.

3. Results

3.1. Patient characteristics

The present study included 40 patients and the number of patients with positive morphology change was 22 (55%). The representative EGMs during the isometric chest press by pressing the palms together are shown in Fig. 1 for both groups of patients. Patient characteristics are summarized in Table 1. There were significant differences in height, sex, New York Heart Association (NYHA) functional class, use of diuretics, and amplitude of the Can-RV coil EGM between the groups.

The ROC curve analysis revealed that 5 mV was an appropriate cut-off point for the Can-RV coil EGM amplitude (Fig. 2), and the area under the curve was estimated to be 0.89.

3.2. Predictors of the positive morphology change during the isometric chest press

Stepwise logistic regression modeling was used to identify factors associated with the positive morphology change incorporating unadjusted variables, which include height ($P=0.0196$), gender ($P=0.0398$), NYHA class ($P=0.023$), use of diuretics ($P=0.0177$), and amplitude of the Can-RV coil EGM less than 5 mV ($P<0.0001$). The results revealed that the candidate predictors were amplitude of the Can-RV coil EGM less than 5 mV ($P<0.0001$) and male sex ($P=0.0212$). The odds ratios determined by the stepwise logistic regression are shown in Fig. 3.

3.3. Inappropriate Wavelet detections caused by myopotential interference

Inappropriate detections caused by myopotential interference occurred in two patients (5%) during the mean follow-up of 49 months (range: 24–92 months). Both of them were classified in

Table 1
Patient characteristics.

	Positive morphology change (n=22)	Negative morphology change (n=18)	P value
Demographics			
Age	63 ± 2.78	60.2 ± 3.99	0.4619
Male	19(86.4)	10(55.6)	0.0398
Height (cm)	165.21 ± 2.57	158.76 ± 2.8	0.0196
Weight (kg)	64.33 ± 3.14	56.62 ± 3.57	0.0505
BMI[a]	23.57 ± 1.86	22.31 ± 1.96	0.2905
Underlying diseases			
Type of heart diseases			
IHD[b]	6(27.3)	5(27.8)	1.0
DCM[c]	1(4.5)	5(27.8)	0.0734
HCM[d]	3(13.6)	3(16.7)	1.0
VHD[e]	0	2(11.1)	0.1962
Myocarditis	0	1(5.6)	0.45
Sarcoidosis	2(9.1)	0	0.4923
CSA[f]	5(22.7)	2(11.1)	0.4271
IVF[g]	5(22.7)	0	0.053
EF[h] **(%)**	51.2 ± 3.76	43.1 ± 3.87	0.099
NYHA[i] **II and more**	5(22.7)	11(61.1)	0.023
Comorbidities			
AF[j]	1(4.5)	3(16.6)	0.31
DM[k]	4(18.2)	5(27.8)	0.7053
HT[l]	6(27.3)	4(22.2)	1.0
DLp[m]	10(45.5)	9(50)	1.0
Hyperuricemia	6(27.3)	4(22.2)	0.6798
Stroke	3(13.6)	4(22.2)	0.381
Medications			
Ia[n]	0	1(5.6)	0.45
Ib[o]	2(9.1)	0	0.4923
Ic[p]	0	0	
Amiodarone	9(41)	8(44.4)	1.0
β blockers	11(50)	14(77.8)	0.104
Ca antagonists	8(36.4)	3(16.7)	0.2863
ACEI/ARB[q]	11(50)	14(77.8)	0.104
Aldosterone antagonist	3(13.6)	4(22.2)	0.6798
Digitalis	0	1(5.6)	0.45
Statins	8(36.4)	7(38.9)	1.0
Nitrates	5(22.7)	1(5.6)	0.1969
Diuretics	3(13.6)	9(50)	0.0177
ICD parameters			
True bipolar ICD lead	15(68.2)	14(77.8)	0.7235
Amplitude of Can-RV coil EGM (mV)	3.9 ± 1.3	7.4 ± 1.6	0.0015

Data are given as means ± SE or n (%).

[a] BMI=body mass index.
[b] IHD=Ischemic heart disease.
[c] DCM=Dilated cardiomyopathy.
[d] HCM=Hypertrophic cardiomyopathy.
[e] VHD=valvular heart disease.
[f] CSA=Coronary spastic angina.
[g] IVF=Idiopathic ventricular fibrillation.
[h] EF=Ejection fraction.
[i] NYHA= The New York Heart Association Functional Classification.
[j] AF= Atrial fibrillation.
[k] DM= diabetes mellitus.
[l] HT=hypertension.
[m] DLp=dyslipidemia.
[n] Ia=Class Ia antiarrhythmic drugs.
[o] Ib= Class Ib antiarrhythmic drugs.
[p] Ic=Class Ic antiarrhythmic drugs.
[q] ACEI/ARB= angiotensin-converting enzyme inhibitor/angiotensin receptor blocker.

the positive morphology change group. The amplitudes of the Can-RV coil EGM of the patients were 2.5 mV and 4 mV, respectively. The EGM recorded during the inappropriate detection is given in Fig. 4A. The Wavelet algorithm interpreted as VT at the time of the Can-RV coil EGM recording is marked by a red circle (Fig. 4A). We interpreted this as sinus tachycardia because the EGM morphology during the tachycardia without myopotential interference was similar to that during sinus rhythm (Fig. 4B). Fig. 4C shows the

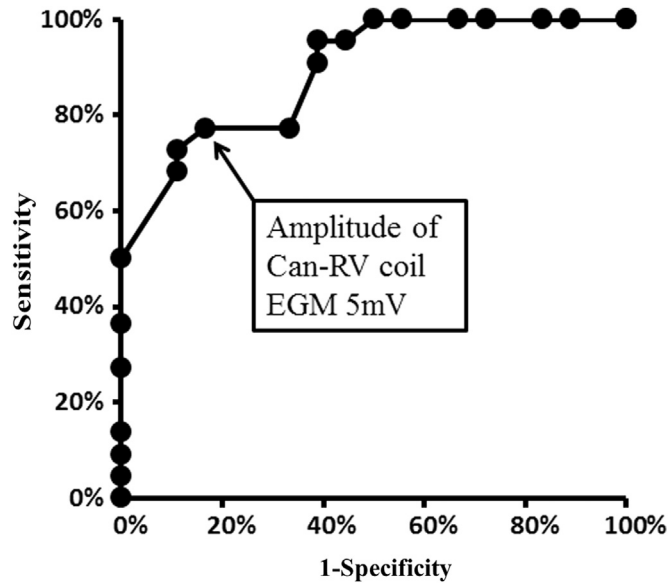

Fig. 2. Receiver operating characteristics (ROC) curve of amplitude of Can-RV coil EGM for positive morphology change during the isometric chest press. The ROC curve indicated the cut-off point at 5 mV.

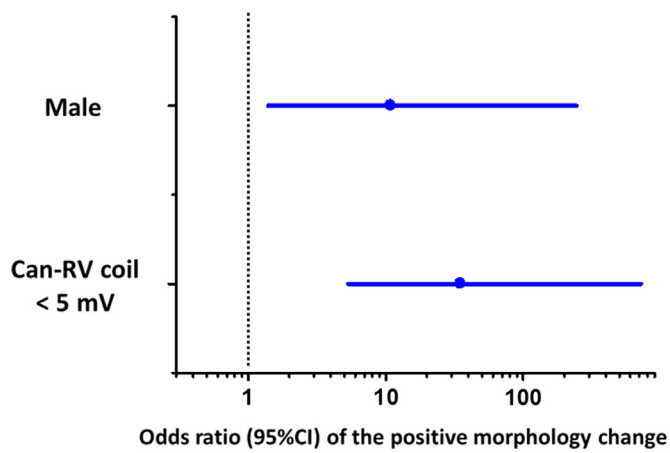

Fig. 3. Odds ratios of the positive morphology change determined by a stepwise logistic regression model for possible factors associated with the induction of myopotential interference.

percent-match score of the Can-RV coil EGM (marked by a red circle in Fig. 4A) on the Wavelet algorithm. The Wavelet recognized this tachycardia as VT since the percent-match score was lower than the threshold (70%).

Another example of inappropriate detection is given in Fig. 5. Before the detection, this tachycardia was irregular (Fig. 5A). The EGM configuration of RV tip-RV ring (Fig. 5A) was similar to that during sinus rhythm (not shown). Therefore, we interpreted this tachycardia as atrial fibrillation. Similar to the result in Fig. 4C, the percent-match score was lower than 70% (Fig. 5C), and the Wavelet algorithm regarded this tachycardia as VT. After a series of ineffective anti-tachycardia pacing, an inappropriate ICD shock was delivered (Fig. 5B), which occurred when the patient was running.

3.4. Tachycardia episodes during follow-up

Ninety episodes of tachycardia were detected in 15 patients during follow-up. The relationship between true rhythm and delivery of ICD shocks is summarized in Table 2. Among the 53 non-VT/VF tachycardia episodes, the myopotential interference

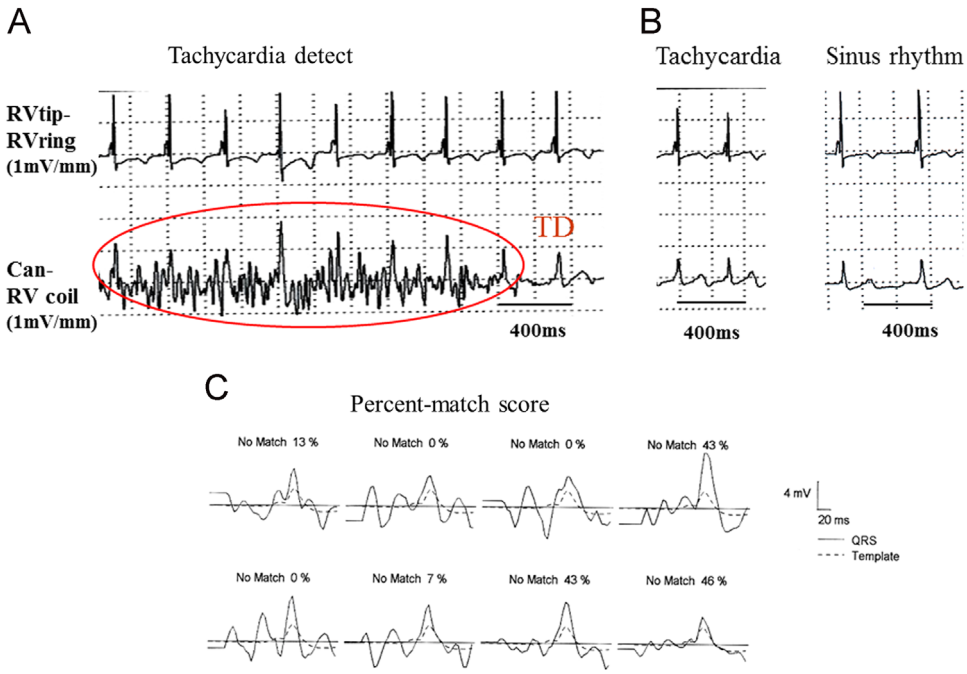

Fig. 4. Inappropriate detection during sinus tachycardia. (A) The EGM recorded at the time of an inappropriate detection. The Wavelet algorithm interpreted as VT when the Can-RV coil EGM marked by a red circle was recorded. (B) The EGM morphology during tachycardia without myopotential noise (left) was similar to that during sinus rhythm (right). (C) The percent-match score of the Can-RV coil EGM in Fig. 4A (marked by a red circle) is shown in each ventricular activation. The percent-match score was lower than the threshold (70%). TD = tachycardia detection.

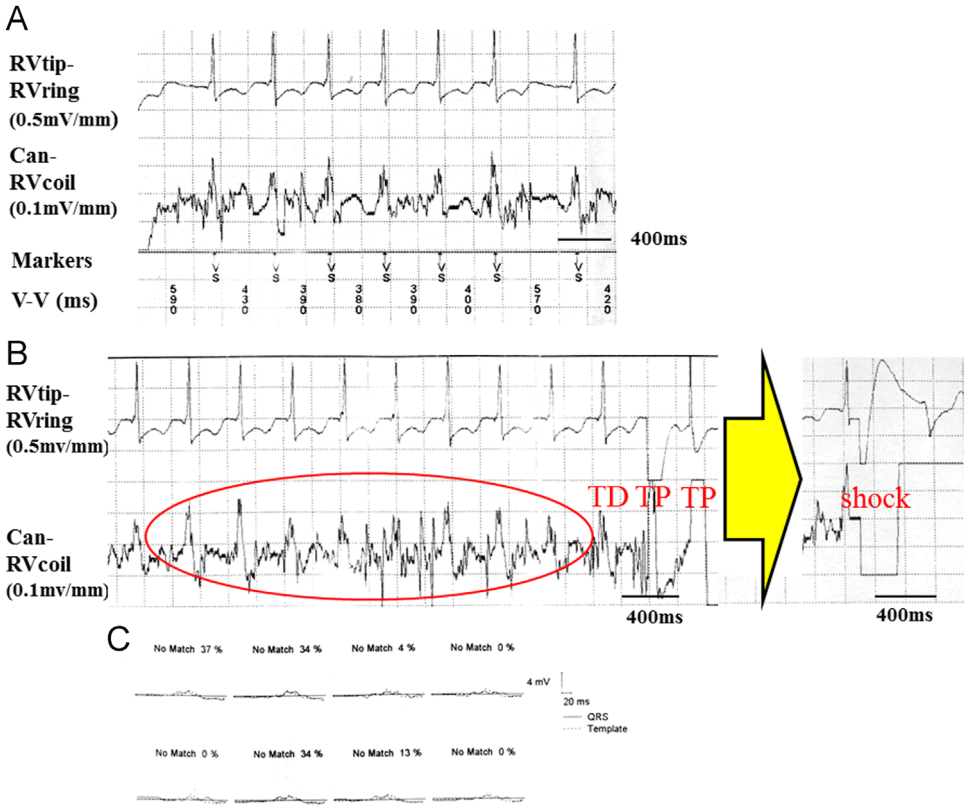

Fig. 5. Inappropriate detection during atrial fibrillation. (A) Immediately before the detection, the cycle length of this tachycardia was irregular. (B) The EGM recorded at the time of an inappropriate detection. The Wavelet algorithm interpreted as VT when the Can-RV coil EGM marked by a red circle was recorded. After a series of ineffective anti-tachycardia pacing, an inappropriate ICD shock was delivered. (C) The percent-match score of the Can-RV coil EGM at the red circle on the Wavelet algorithm. The percent-match score was lower than the threshold (70%). TD = tachycardia detection; TP = anti-tachycardia pacing.

Table 2
Relationship between true rhythm and ICD therapy.

True rhythm			
Delivery of ICD shocks		**VT/VF**	**Non-VT/VF**
	Yes	**37 Episodes (7 Patients)**	**16 Episodes[a] (7 Patients)**
	No	**0 Episodes (0 Patients)**	**37 Episodes (5 Patients)**

[a] Seven episodes faster than the supraventricular tachycardia (SVT) limit due to T-wave oversensing and/or SVT (two patients) and nine episodes due to the wavelet misclassification during SVT (five patients) were included. Among these nine episodes, one inappropriate ICD shock was delivered because of the morphology change by myopotential interference (Fig. 5).

occurred during two episodes in two patients (Figs. 4 and 5). An ICD shock was withheld at the episode in a former patient because of its short duration. The incidence rate of the myopotential noise leading to the Wavelet misclassification was 3.8% (two of 53 episodes) in the clinical setting. The incidence rate of misclassification by the myopotential interference was 11.1% (one of nine episodes) in the presence of atrial fibrillation and 2.3% (one of 44 episodes) in the absence of atrial fibrillation ($P=0.205$).

ICD shocks were delivered to 53 out of 90 episodes (Table 2). These included 37 appropriate ICD shocks in seven patients and 16 inappropriate ICD shocks in seven patients. Positive and negative predictive accuracy rates for appropriate ICD discharges were 69.8% and 100%, respectively, while sensitivity and specificity performance rates were 100% and 69.8%, respectively. Among the 16 inappropriate ICD shocks, the reasons for misdiagnosis were (a) the events faster than the SVT limit (including T-wave oversensing) in seven episodes and (b) the Wavelet misclassification due to morphological changes of EGM in nine episodes, which included an episode affected by the myopotential interference (Fig. 5). Therefore, the inappropriate ICD shock due to myopotential interference on the Wavelet algorithm accounted for 6.3% (one out of 16 episodes) among all the inappropriate ICD shocks in this series of patients.

4. Discussion

The present study has demonstrated that the Wavelet discrimination algorithm is affected by myopotential interference, as evidenced by the large number of patients (55%) showing positive morphology change (defined as the percent-match score of the Wavelet less than 70%) during the isometric chest press by pressing the palms together. In fact, inappropriate tachycardia detections induced by myopotential interference occurred in two patients (5%) during a mean follow-up period of 49 months. Further, amplitude of the Can-RV coil EGM less than 5 mV and male sex were candidate predictors of positive morphology change.

A previous study reported that the use of the morphology discrimination algorithm alone was effective in terms of differentiation of SVT from VT [27]. Later studies demonstrated that the advanced morphology-based algorithms reduced inappropriate therapy without decrease in the sensitivity of VT [18,28]. More recently, it was reported that the tachycardia discrimination using Wavelet was excellent [29,30]. The START study reported that the specificity rate for rejection of 50 atrial arrhythmias was 92% in single-chamber ICDs equipped with the Wavelet algorithm [29]. However, the atrial arrhythmias were induced in the electrophysiological laboratory by programmed stimulation or burst pacing in the supine position [29]. Further, PainFree SST (SmartShock™ technology algorithms) trial, a large patient cohort study receiving ICDs, has underscored the usefulness of novel discrimination algorithms (including the Wavelet) with modern programming strategies in terms of reducing inappropriate shocks of less than 3% at 1 year [30]. In this trial, the most frequent cause of an inappropriate shock was atrial fibrillation, followed by oversensing due to EGM noise. Thus, it is important to note that EGM noise is a critical cause of inappropriate shocks even in the use of modern ICD devices.

Previous studies reported that inappropriate detections caused by myopotential interference were observed in Section 2.3 − 5% of patients using the Wavelet algorithm [18,21,22]. This is similar to the present study showing that the rate of inappropriate detections was 5% (2 of 40 patients). In fact, one patient received an inappropriate shock due to the Wavelet misclassification produced by myopotential interference (Fig. 5). Therefore, we should consider the possibility of myopotential noise interfering with the Wavelet algorithm that could result in the misclassification of tachycardia episodes in a small number of patients. However, no study has identified factors associated with myopotential interference in the Wavelet algorithm to date.

To our knowledge, the present study is the first to demonstrate that (a) Can-RV coil EGM amplitude less than 5 mV and (b) male sex would be independent predictors of positive morphology change caused by myopotential interference (Fig. 3). The fusion of myopotential noise to the Can-RV coil EGM could affect the morphology of the true ventricular electrogram. When the amplitude of the Can-RV coil EGM is smaller, the relative influence of the myopotential noise would be larger, thereby leading to lower percent-match scores in the Wavelet algorithm. As the nominal Can-RV coil EGM of the Wavelet algorithm derives from far-field potentials, it might be influenced by muscular mass and strength. Thus, patients with morphology change appear to have high physical activity level with muscularity. We should recognize that such patients might be more susceptible to myopotential interference when the amplitude of the Can-RV coil EGM is less than 5 mV.

Changing the EGM source of the wavelet algorithm may be one of the methods to resolve myopotential interference. We did not use the near-field EGM on the Wavelet algorithm because it reduced the sensitivity for VT detection [20,21]. Among the far-field EGM configurations, either Can-SVC coil or RV coil-SVC coil configurations can be selected. However, the morphology of the Can-SVC coil EGM is likely to be influenced by an increase in heart rate and changes in posture [23,24], whereas that of the RV coil-SVC coil EGM is stable during postural change [24]. At present, no comparative data between RV coil-SVC coil EGM and Can-RV coil EGM are available. Whether or not a more sophisticated algorithm [31] could reduce inappropriate detections due to myopotential interference requires further investigations.

4.1. Study limitations

First, this was a single-center retrospective study, which might, therefore, incorporate important biases. Second, the sample size was small. Third, there are other morphology discrimination algorithms used other than Wavelet. Thus, further studies are required to achieve the best diagnostic accuracy in ICD therapy.

5. Conclusions

Wavelet algorithm is an effective tool for the discrimination of tachycardia. However, it is affected by myopotential interference, which can lead to inappropriate detections. Thus, we should keep this drawback in mind when results reveal a Can-RV coil EGM amplitude of less than 5 mV. To reduce inappropriate ICD therapies, it is recommended that we assess the level of physical

activity, presence or absence of SVT and slow VT, ICD indication such as primary or secondary prevention, and amplitude of EGM source when the wavelet algorithm is operative. After these assessments, we should determine the programming parameters and tachycardia discrimination algorithms in patients with ICDs.

Conflict of interest

All authors declare no conflict of interest related to this study.

Acknowledgments

We thank Dr. Masayuki Sakurai, Director of Hokko Memorial Hospital, for constant encouragement of this study.

References

[1] A comparison of antiarrhythmic-drug therapy with implantable defibrillators in patients resuscitated from near-fatal ventricular arrhythmias. The Antiarrhythmics versus Implantable Defibrillators (AVID) Investigators. N Engl J Med;1997;337:1576–83.
[2] Klein H, Auricchio A, Reek S, et al. New primary prevention trials of sudden cardiac death in patients with left ventricular dysfunction: SCD-HEFT and MADIT-II. Am J Cardiol 1999;83:91D–97DD.
[3] Lee DS, Green LD, Liu PP, et al. Effectiveness of implantable defibrillators for preventing arrhythmic events and death: a meta-analysis. J Am Coll Cardiol 2003;41:1573–82.
[4] Nanthakumar K, Epstein AE, Kay GN, et al. Prophylactic implantable cardioverter-defibrillator therapy in patients with left ventricular systolic dysfunction: a pooled analysis of 10 primary prevention trials. J Am Coll Cardiol 2004;44:2166–72.
[5] van Rees JB, Borleffs CJ, de Bie MK, et al. Inappropriate implantable cardioverter-defibrillator shocks: incidence, predictors, and impact on mortality. J Am Coll Cardiol 2011;57:556–62.
[6] Tenma T, Yokoshiki H, Mizukami K, et al. Predictors and proarrhythmic consequences of inappropriate implantable cardioverter-defibrillator therapy. Circ J 2015;79:1920–7.
[7] Poole JE, Johnson GW, Hellkamp AS, et al. Prognostic importance of defibrillator shocks in patients with heart failure. N Engl J Med 2008;359:1009–17.
[8] Daubert JP, Zareba W, Cannom DS, et al. Inappropriate implantable cardioverter-defibrillator shocks in MADIT II: frequency, mechanisms, predictors, and survival impact. J Am Coll Cardiol 2008;51:1357–65.
[9] Wilkoff BL, Kuhlkamp V, Volosin K, et al. Critical analysis of dual-chamber implantable cardioverter-defibrillator arrhythmia detection: results and technical considerations. Circulation 2001;103:381–6.
[10] Friedman PA, McClelland RL, Bamlet WR, et al. Dual-chamber versus single-chamber detection enhancements for implantable defibrillator rhythm diagnosis: the detect supraventricular tachycardia study. Circulation 2006;113:2871–9.
[11] Neuzner J, Pitschner HF, Schlepper M. Programmable VT detection enhancements in implantable cardioverter defibrillator therapy. Pacing Clin Electrophysiol 1995;18:539–47.
[12] Schaumann A, von zur Muhlen F, Gonska BD, et al. Enhanced detection criteria in implantable cardioverter-defibrillators to avoid inappropriate therapy. Am J Cardiol 1996;78:42–50.
[13] Sears SF, Lewis TS, Kuhl EA, et al. Predictors of quality of life in patients with implantable cardioverter defibrillators. Psychosomatics 2005;46:451–7.
[14] Schron EB, Exner DV, Yao Q, et al. Quality of life in the antiarrhythmics versus implantable defibrillators trial: impact of therapy and influence of adverse symptoms and defibrillator shocks. Circulation 2002;105:589–94.
[15] Pinski SL, Fahy GJ. The proarrhythmic potential of implantable cardioverter-defibrillators. Circulation 1995;92:1651–64.
[16] Healy E, Goyal S, Browning C, et al. Inappropriate ICD therapy due to proarrhythmic ICD shocks and hyperpolarization. Pacing Clin Electrophysiol 2004;27:415–6.
[17] Vollmann D, Luthje L, Vonhof S, et al. Inappropriate therapy and fatal proarrhythmia by an implantable cardioverter-defibrillator. Heart Rhythm 2005;2:307–9.
[18] Klein GJ, Gillberg JM, Tang A, et al. Improving SVT discrimination in single-chamber ICDs: a new electrogram morphology-based algorithm. J Cardiovasc Electrophysiol 2006;17:1310–9.
[19] Toquero J, Alzueta J, Mont L, et al. Morphology discrimination criterion wavelet improves rhythm discrimination in single-chamber implantable cardioverter-defibrillators: Spanish Register of morphology discrimination criterion wavelet (REMEDIO). Europace 2009;11:727–33.
[20] Koyrakh LA, Gillberg JM, Wood NM. Wavelet transform based algorithms for EGM morphology discrimination for implantable ICDs. Comput Cardiol 1999;26:343–6.
[21] Compton SJ, Merrill JJ, Dorian P, et al. Continuous template collection and updating for electrogram morphology discrimination in implantable cardioverter defibrillators. Pacing Clin Electrophysiol 2006;29:244–54.
[22] Swerdlow CD, Brown ML, Lurie K, et al. Discrimination of ventricular tachycardia from supraventricular tachycardia by a downloaded wavelet-transform morphology algorithm: a paradigm for development of implantable cardioverter defibrillator detection algorithms. J Cardiovasc Electrophysiol 2002;13:432–41.
[23] Luthje L, Vollmann D, Rosenfeld M, et al. Electrogram configuration and detection of supraventricular tachycardias by a morphology discrimination algorithm in single chamber ICDs. Pacing Clin Electrophysiol 2005;28:555–60.
[24] Wolber T, Binggeli C, Holzmeister J, et al. Wavelet-based tachycardia discrimination in ICDs: impact of posture and electrogram configuration. Pacing Clin Electrophysiol 2006;29:1255–60.
[25] Lau CP, Linker NJ, Butrous GS, et al. Myopotential interference in unipolar rate responsive pacemakers. Pacing Clin Electrophysiol 1989;12:1324–30.
[26] Jain P, Kaul U, Wasir HS. Myopotential inhibition of unipolar demand pacemakers: utility of provocative manoeuvres in assessment and management. Int J Cardiol 1992;34:33–9.
[27] Boriani G, Occhetta E, Pistis G, et al. Combined use of morphology discrimination, sudden onset, and stability as discriminating algorithms in single chamber cardioverter defibrillators. Pacing Clin Electrophysiol 2002;25:1357–66.
[28] Lee MA, Corbisiero R, Nabert DR, et al. Clinical results of an advanced SVT detection enhancement algorithm. Pacing Clin Electrophysiol 2005;28:1032–40.
[29] Gold MR, Theuns DA, Knight BP, et al. Head-to-head comparison of arrhythmia discrimination performance of subcutaneous and transvenous ICD arrhythmia detection algorithms: the START study. J Cardiovasc Electrophysiol 2012;23:359–66.
[30] Auricchio A, Schloss EJ, Kurita T, et al. Low inappropriate shock rates in patients with single- and dual/triple-chamber implantable cardioverter-defibrillators using a novel suite of detection algorithms: PainFree SST trial primary results. Heart Rhythm 2015;12:926–36.
[31] Auricchio A, Meijer A, Kurita T, et al. Safety, efficacy, and performance of new discrimination algorithms to reduce inappropriate and unnecessary shocks: the PainFree SST clinical study design. Europace 2011;13:1484–93.